*Journal of the Korean Chemical Society*
**2024**, *Vol. 68, No. 2*
Printed in the Republic of Korea
https://doi.org/10.5012/jkcs.2024.68.2.65

# Theoretical Investigation of the Hydrogen-bonded Halide-acetylene Anion Complexes

**Byeong-Seo Cheong**
*Department of Chemistry, Incheon National University, Incheon 22012, Korea.*
*E-mail: bcheong@inu.ac.kr*
(Received February 15, 2024; Accepted March 21, 2024)

**ABSTRACT.** The halide-acetylene anions, $X^-$–HCCH (X = F, Cl, and Br) have been studied by using several different *ab initio* and DFT methods to determine structures, hydrogen-bond energies, vibrational frequencies of the anion complexes. Although the halide-acetylene complexes all have linear equilibrium structures, it is found that the fluoride complex is characterized with distinctively different structure and interactions compared to those of the chloride and bromide complexes. The performance of various density functionals on describing ionic hydrogen-bonded complexes is assessed by examining statistical deviations with respect to high level *ab initio* CCSD(T) results as reference. The density functionals employed in the present work show considerably varying degrees of performance depending on the properties computed. The performances of each density functional on geometrical parameters related with the hydrogen bond, hydrogen-bond energies, and scaled harmonic frequencies of the anion complexes are examined and discussed based on the statistical deviations.

**Key words:** Halide-acetylene complex, Hydrogen-bonding, Hydrogen-bond energy, Vibrational frequencies, DFT

## INTRODUCTION

Hydrogen bonds are important for the structure, function, solvation, and dynamics of a large number of chemical systems in many fields of chemistry and biological science.[1,2] As a special case of hydrogen bonds, ionic hydrogen bonds that form between ions and molecules are particularly interesting.[3] The binding energies of ionic hydrogen-bonded complexes exceed considerably the binding energies of 3–10 kcal/mol for neutral hydrogen-bonded complexes, thus possessing significant covalent character. These strong interactions play important roles in ion solvation, nucleation, electrolytes, protein folding, formation of membrane and proton transport, and the low barrier hydrogen bond in enzymatic catalysis, etc.[3]

Owing to their importance in chemistry and biological science, hydrogen bonds have been a subject of numerous theoretical and computational studies.[4,5] Traditional *ab initio* methodologies such as Møller-Plesset perturbation theory or coupled-cluster theory have been quite successful in describing hydrogen bonding interactions. With the recent advancement in density functional theory (DFT) and development of a wide range of density functionals,[6] the DFT methods have become a popular alternative to the wave function-based methods and efforts have been made to apply DFT to the hydrogen-bonded systems. However, the density functionals developed earlier have not been successful in describing nonbonded interactions partly because dispersion attraction and long-range interactions are not treated properly in these functionals. As much efforts continue to be made in treating nonbonded interactions by the first principle quantum chemical methods, many new functionals including range-separated functionals and dispersion-corrected functionals have been developed with the aim of accurate description of hydrogen bonding interactions.[6-8]

Among many ionic hydrogen-bonded complexes, the complexes between halide ions and small proton donor molecules such as water and alcohols have been extensively studied experimentally and theoretically.[9-12] On the other hand, the complexes of halide ions with the ammonia or acetylene molecule, which have relatively small binding energies due to the low acidity of ammonia or acetylene, have received much less attention. Recently our group became interested in these ionic hydrogen-bonded complexes, and reported a study of the halide-ammonia anion complexes.[13] As a continuation of previous study, we have investigated here the halide-acetylene anion complexes as a model system of ionic hydrogen bonds.

A few spectroscopic studies have been reported for the halide-acetylene anions. Bieske and coworkers studied the chloride-, bromide-, and iodide-acetylene anion complexes using vibrational predissociation spectroscopy.[14-16] These halide-acetylene complexes were also investigated by anion

photoelectron spectroscopy.[17] Theoretically, large scale *ab initio* calculations at the MP2 and CCSD(T) levels using large basis sets have been carried out for the complexes of heavier halide ions.[18,19] However, there is little computational study of applying the DFT method to these anions. Denis and Gancheff have investigated hydrogen bonds between halides and a few proton donors including acetylene by coupled cluster and density functional calculations.[20]

In the present work, we have investigated the hydrogen-bonded halide-acetylene anion complexes, $X^-$–HCCH (X = F, Cl, and Br) by using both *ab initio* and density functional theory (DFT) methods. The molecular structures, hydrogen-bond energies, vibrational frequencies of the complexes were calculated to obtain consistent sets of data at sufficiently high levels for all three anions. In addition, attempts were made to assess the performance of various density functionals on the ionic hydrogen-bonded complexes and the results calculated with each density functional were evaluated by comparing the statistical deviations relative to the results of *ab initio* CCSD(T) calculations.

## COMPUTATIONAL

The halide-acetylene anion complexes were investigated using both *ab initio* and DFT methods. *Ab initio* calculations were performed at the coupled cluster, CCSD(T) and second-order Møller–Plesset (MP2) levels. For DFT calculations, several different density functionals and dispersion corrections were employed. B97-D[21] is the generalized gradient approximation (GGA) functional, B3LYP[22] and PBE1PBE (also known as PBE0)[23] the hybrid GGA functionals, and M06-2X[24] the hybrid meta-GGA functional. CAM-B3LYP,[25] LC-ωHPBE,[26] and ωB97X-D[27] are the range-separated functionals that include long-range corrections. LC-BLYP is another long-range corrected functional for which the long-range correction scheme of Hirao and coworkers[28] is applied to the pure BLYP functional. The long-range corrections attempt to remedy the deficiency of the non-Coulomb part of exchange functionals diminishing too quickly and thus becoming very inaccurate at large distances. For dispersion corrections,[29] the D3 correction was included in B3LYP-D3, while B97-D and ωB97X-D functionals have a built-in dispersion term. The sufficiently large aug-cc-pVTZ basis set was used to minimize the basis set effects.

In the present study, the hydrogen-bond energy of the anion complexes is defined as the energy change in the dissociation reaction of $X^-$–HCCH into its constituents with the zero-point energy correction included:

$$X^- - HCCH(g) \rightarrow X^-(g) + HCCH(g) \quad (1)$$

In addition, the counterpoise correction was also included to take account into the basis set superposition error (BSSE).[30,31] The hydrogen-bond energies were also estimated by using the W1BD[32] and G4[33] composite methods. These composite methods use extrapolation scheme to yield highly accurate thermochemical data.

All calculations were performed using the Gaussian 16 program package.[34] The geometries of the anion complexes were fully optimized with no constraint with "tight" convergence criteria, and DFT calculations were conducted using the "ultrafine" grid. Each optimized structure was characterized by harmonic vibrational frequency calculations either analytically or numerically.

In order to assess the performance of various density functionals for the anion complexes on the statistical grounds, three different deviations, that is, mean absolute deviation (MAD), mean signed deviation (MSD), and mean absolute percent deviation (MAPD) were computed on the DFT calculated results with respect to the reference value. The main difference between MAD and MAPD is that MAPD is more sensitive in those cases with smaller values in the reference. For MSD, the negative number indicates that the DFT calculated value is lower than the reference value. Since there is little experimental data available for the $X^-$–HCCH complexes, the deviations were calculated relative to the *ab initio* CCSD(T) results as reference.

## RESULTS AND DISCUSSION

The optimized equilibrium geometries of the halide-acetylene anions, $X^-$–HCCH (X = F, Cl, and Br) are presented in *Table* 1 and the structures of anions optimized at the CCSD(T) level are shown in *Fig*. 1. In *Table* 1 and thereafter, the H-bonded hydrogen is denoted with the *

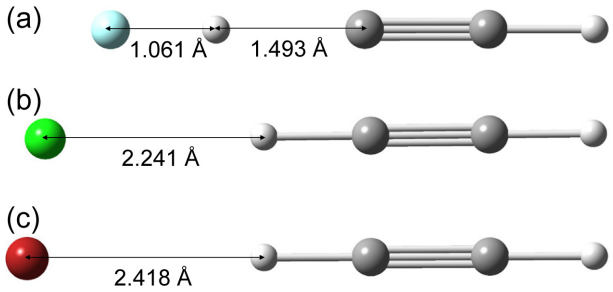


***Figure* 1.** Structures of the $X^-$–HCCH anion complexes optimized at the CCSD(T) level. (a) X = F, (b) X = Cl, (c) X = Br

***Table* 1.** Optimized geometries of the $X^-$–HCCH complexes (X= F, Cl, and Br)

| Method | Total energy (hartree) | R(X–H*)[a] (Å) | R(H*–C)[a] (Å) | R(C–C) (Å) | R(C–H) (Å) | ΔR(H*–C)[b] (Å) |
|---|---|---|---|---|---|---|
| | | | $F^-$–HCCH | | | |
| CCSD(T) | −176.9865390 | 1.061 | 1.493 | 1.240 | 1.068 | 0.429 |
| MP2 | −176.9470930 | 1.125 | 1.395 | 1.239 | 1.065 | 0.333 |
| B97-D | −177.1893163 | 1.196 | 1.340 | 1.230 | 1.070 | 0.274 |
| B3LYP | −177.2970976 | 1.319 | 1.229 | 1.215 | 1.062 | 0.168 |
| B3LYP-D3 | −177.2981112 | 1.331 | 1.225 | 1.215 | 1.062 | 0.163 |
| PBE1PBE | −177.0884706 | 1.121 | 1.399 | 1.223 | 1.066 | 0.335 |
| M06-2X | −177.2226307 | 1.057 | 1.506 | 1.222 | 1.065 | 0.443 |
| CAM-B3LYP | −177.2243303 | 1.309 | 1.231 | 1.209 | 1.062 | 0.169 |
| LC-ωHPBE | −177.1698266 | 1.279 | 1.253 | 1.208 | 1.065 | 0.188 |
| LC-BLYP | −176.8966563 | 1.334 | 1.213 | 1.198 | 1.062 | 0.150 |
| ωB97X-D | −177.2272415 | 1.144 | 1.374 | 1.219 | 1.064 | 0.311 |
| | | | $Cl^-$–HCCH | | | |
| CCSD(T) | −537.0168414 | 2.241 | 1.093 | 1.216 | 1.063 | 0.029 |
| MP2 | −536.9638344 | 2.224 | 1.092 | 1.218 | 1.061 | 0.030 |
| B97-D | −537.6392497 | 2.279 | 1.100 | 1.212 | 1.066 | 0.033 |
| B3LYP | −537.6907649 | 2.277 | 1.092 | 1.202 | 1.061 | 0.031 |
| B3LYP-D3 | −537.6923416 | 2.277 | 1.092 | 1.202 | 1.061 | 0.030 |
| PBE1PBE | −537.4103882 | 2.209 | 1.099 | 1.203 | 1.063 | 0.035 |
| M06-2X | −537.6175843 | 2.264 | 1.091 | 1.200 | 1.062 | 0.029 |
| CAM-B3LYP | −537.6388568 | 2.267 | 1.091 | 1.197 | 1.061 | 0.029 |
| LC-ωHPBE | −537.4741081 | 2.262 | 1.094 | 1.196 | 1.061 | 0.029 |
| LC-BLYP | −537.1649207 | 2.251 | 1.092 | 1.188 | 1.062 | 0.029 |
| ωB97X-D | −537.6337622 | 2.271 | 1.093 | 1.200 | 1.061 | 0.031 |
| | | | $Br^-$–HCCH | | | |
| CCSD(T) | −2650.0020651 | 2.418 | 1.088 | 1.215 | 1.063 | 0.024 |
| MP2 | −2649.9559703 | 2.398 | 1.087 | 1.218 | 1.061 | 0.026 |
| B97-D | −2652.9218560 | 2.545 | 1.091 | 1.210 | 1.066 | 0.024 |
| B3LYP | −2651.6957003 | 2.518 | 1.085 | 1.201 | 1.061 | 0.024 |
| B3LYP-D3 | −2651.6975004 | 2.516 | 1.085 | 1.201 | 1.061 | 0.023 |
| PBE1PBE | −2651.2556989 | 2.444 | 1.091 | 1.202 | 1.063 | 0.027 |
| M06-2X | −2651.6643178 | 2.500 | 1.085 | 1.199 | 1.062 | 0.022 |
| CAM-B3LYP | −2651.7423862 | 2.503 | 1.085 | 1.196 | 1.061 | 0.023 |
| LC-ωHPBE | −2651.2348789 | 2.497 | 1.088 | 1.195 | 1.064 | 0.022 |
| LC-BLYP | −2651.0274910 | 2.477 | 1.086 | 1.187 | 1.062 | 0.022 |
| ωB97X-D | −2651.6871063 | 2.513 | 1.086 | 1.199 | 1.061 | 0.024 |

[a]The symbol * denotes the H-bonded hydrogen.
[b]Changes relative to the C-H bond length in the free HCCH molecule

symbol. All halide-acetylene anion complexes were found to have a linear configuration at the ground state. As shown in *Fig.* 1, however, the fluoride-acetylene anion formed a different structure compared to the other two anions. The geometrical parameters optimized at the CCSD(T) level suggested that the structure of the fluoride anion complex nearly corresponds to the complex between F-H and $CCH^-$ instead of between fluoride ion and acetylene. The distance of 1.061 Å between the F and H atoms is quite short, rather close to the bond length of 0.92 Å for the free HF molecule. This type of structure for the fluoride complex has also been suggested in previous computational studies.[18,20] The structures of the chloride and bromide complexes were formed by the interaction between $X^-$ and HCCH, as indicated by large separation between the X and H atoms.

While different density functionals examined in the

***Table* 2.** Statistical analysis of the X–H* and C–H* bond lengths calculated for $X^-$–HCCH relative to the CCSD(T) values

| Method | MAD (Å) | MSD (Å) | MAPD (%) |
|---|---|---|---|
| MP2 | 0.033 | –0.012 | 2.4 (6.3)[a] |
| B97-D | 0.077 | 0.026 | 5.1 (11.5) |
| B3LYP | 0.110 | 0.021 | 8.0 (21.0) |
| B3LYP-D3 | 0.113 | 0.022 | 8.3 (21.7) |
| PBE1PBE | 0.037 | –0.005 | 2.6 (6.0) |
| M06-2X | 0.021 | 0.018 | 1.0 (0.6) |
| CAM-B3LYP | 0.104 | 0.015 | 7.7 (20.5) |
| LC-ωHPBE | 0.093 | 0.013 | 6.8 (18.4) |
| LC-BLYP | 0.104 | 0.010 | 8.0 (22.2) |
| ωB97X-D | 0.055 | 0.014 | 3.6 (7.9) |

[a]The numbers in parentheses are obtained using the results on the fluoride complex only.

present work predicted similar structures as the CCSD(T) method for the chloride- and bromide-acetylene complexes, the geometry of the fluoride complex varied significantly depending on density functionals employed. As shown in *Table* 1, the geometrical parameters for the fluoride complex obtained with the M06-2X functional were very close to those obtained with the CCSD(T) method, but other functionals exhibited varying degrees of agreement with the geometry predicted by the CCSD(T) method. In particular, the B3LYP and related functionals predicted considerably longer F–H* and shorter H*–C bond lengths.

*Table* 2 presents statistical deviations computed on the geometrical parameters optimized using various density functionals with respect to the CCSD(T) values. Only the bond lengths related with hydrogen bonding, that is, the X–H* and C–H* bond lengths were included in computation of deviations. However, these statistical deviations were most significantly affected by the results on the fluoride complex, and therefore separate analysis was performed only with the results on the fluoride complex and the MAPD values were also listed in *Table* 2. As shown in *Table* 2, most density functionals yielded longer X–H* and C–H* bond lengths than the CCSD(T) method predicted, as indicated by the positive sign in MSDs. As already seen in *Table* 1, the M06-2X functional yielded the smallest deviations, and the PBE1PBE and ωB97X-D functionals also resulted in relatively small deviations compared to other functionals. On the other hand, the B3LYP, B3LYP-D3, LC-BLYP, and CAM-B3LYP functionals showed rather poor performance as shown in *Table* 2. Thus, it appears that dispersion correction or range-separated functionals are not particularly effective in improving geometrical parame-

***Table* 3.** Hydrogen-bond energy $\Delta E_0$ in kcal/mol of the $X^-$–HCCH complexes (X = F, Cl, and Br)

| Method | $\Delta E_{elec}$ | ΔZPE | $\Delta E_{CP}$ | $\Delta E_0$ |
|---|---|---|---|---|
| | | $F^-$–HCCH | | |
| CCSD(T) | 24.42 | 0.70 | –1.85 | 23.27 (25.12)[a] |
| MP2 | 23.32 | 1.56 | –1.73 | 23.14 (24.87) |
| B97-D | 23.49 | 1.86 | –0.52 | 24.82 (25.35) |
| B3LYP | 23.01 | 1.22 | –0.27 | 23.96 (24.23) |
| B3LYP-D3 | 23.46 | 1.11 | –0.27 | 24.30 (24.57) |
| PBE1PBE | 26.21 | 1.42 | –0.26 | 27.38 (27.63) |
| M06-2X | 27.54 | 0.55 | –0.21 | 27.88 (28.09) |
| CAM-B3LYP | 23.71 | 1.22 | –0.20 | 24.72 (24.92) |
| LC-ωHPBE | 22.68 | 1.39 | –0.18 | 23.89 (24.08) |
| LC-BLYP | 24.35 | 0.88 | –0.15 | 25.08 (25.23) |
| ωB97X-D | 23.97 | 1.92 | –0.23 | 25.66 (25.89) |
| G4 | 21.79 | | | 23.96 |
| W1BD | 23.48 | | | 24.26 |
| Other works | | | | 24.1[b] |
| | | $Cl^-$–HCCH | | |
| CCSD(T) | 11.31 | –0.56 | –0.90 | 9.85 (10.75)[a] |
| MP2 | 11.44 | –0.52 | –0.91 | 10.02 (10.92) |
| B97-D | 10.15 | –0.25 | –0.13 | 9.78 (9.90) |
| B3LYP | 9.84 | –0.37 | –0.11 | 9,36 (9,47) |
| B3LYP-D3 | 10.63 | –0.36 | –0.11 | 10.16 (10.27) |
| PBE1PBE | 11.07 | –0.33 | –0.10 | 10.64 (10.74) |
| M06-2X | 10.88 | –0.43 | –0.18 | 10.27 (10.44) |
| CAM-B3LYP | 10.27 | –0.42 | –0.11 | 9.74 (9.85) |
| LC-ωHPBE | 9.97 | –0.43 | –0.12 | 9.42 (9.54) |
| LC-BLYP | 10.98 | –0.47 | –0.15 | 10.36 (10.51) |
| ωB97X-D | 10.40 | –0.38 | –0.10 | 9.92 (10.02) |
| G4 | 10.52 | | | 10.47 |
| W1BD | 10.70 | | | 10.49 |
| Other works | | | | 10.9[b], 10.3[c] |
| | | $Br^-$–HCCH | | |
| CCSD(T) | 10.47 | –0.60 | –1.88 | 7.99 (9.87)[a] |
| MP2 | 10.72 | –0.56 | –1.94 | 8.22 (10.16) |
| B97-D | 8.64 | –0.26 | –0.16 | 8.23 (8.39) |
| B3LYP | 7.99 | –0.35 | –0.12 | 7.53 (7.65) |
| B3LYP-D3 | 8.93 | –0.34 | –0.12 | 8.47 (8.59) |
| PBE1PBE | 9.10 | –0.33 | –0.12 | 8.66 (8.78) |
| M06-2X | 9.04 | –0.41 | –0.20 | 8.43 (8.63) |
| CAM-B3LYP | 8.39 | –0.40 | –0.12 | 7.87 (7.99) |
| LC-ωHPBE | 8.21 | –0.41 | –0.14 | 7.65 (7.80) |
| LC-BLYP | 9.08 | –0.44 | –0.16 | 8.47 (8.63) |
| ωB97X-D | 8.61 | –0.36 | –0.11 | 8.13 (8.24) |
| G4 | 8.53 | | | 8.24 |
| Other works | | | | 9.1[b], 9.11[c] |
| Expt[d] | | | | 8.63 |

[a]Calculated without counterpoise correction.
[b]CCSD(T)/aug-cc-pVQZ energies, Ref. 20.
[c]CCSD(T)/CBS energies, Ref. 17.
[d]Ref. 15a.

ters of ionic hydrogen-bonded complexes.

*Table* 3 presents the hydrogen-bond energies of the halide-acetylene complexes estimated with zero-point energy and BSSE corrections using various *ab initio* and DFT methods. Also, the hydrogen-bond energies obtained by the W1BD and G4 composite methods are listed for comparison in *Table* 3. As shown in *Table* 3, the hydrogen-bond energies for the fluoride complex were estimated to be quite large in the range of 23–28 kcal/mol, probably due to the formation of the H-F part in the $[F\text{-}H\cdots CCH]^-$ complex. On the other hand, the hydrogen-bond energies for the chloride and bromide complexes were in the range expected from typical hydrogen bonds. It is difficult to determine errors involved in the hydrogen-bonded energies calculated in the present work since there is little experimental energies reported for the halide-acetylene complexes. The dissociation energy only for the bromide anion complex has been reported from vibrational predissociation spectroscopy,[15a] and the dissociation energy of 8.63 kcal/mol is quite close to the hydrogen-bond energies calculated here for the bromide complex. Also, the hydrogen-bond energies estimated from CCSD(T) calculations are in reasonably good agreements with previous CCSD(T) calculations on these anion complexes.[17-20]

***Table* 4.** Statistical analysis of the hydrogen-bond energies of $X^-$–HCCH relative to the CCSD(T) values

| Method | MAD (kcal/mol) | MSD (kcal/mol) | MAPD (%) |
|---|---|---|---|
| MP2 | 0.17 | 0.09 | 1.7 (0.6)[a] |
| B97-D | 0.62 | 0.57 | 3.5 (6.7) |
| B3LYP | 0.55 | –0.09 | 4.6 (3.0) |
| B3LYP-D3 | 0.61 | 0.61 | 4.6 (4.4) |
| PBE1PBE | 1.86 | 1.86 | 11.4 (17.6) |
| M06-2X | 1.82 | 1.82 | 9.9 (19.8) |
| CAM-B3LYP | 0.56 | 0.41 | 2.9 (6.2) |
| LC-ωHPBE | 0.46 | –0.05 | 3.7 (2.7) |
| LC-BLYP | 0.94 | 0.94 | 6.3 (7.8) |
| ωB97X-D | 0.87 | 0.87 | 4.3 (10.3) |

[a]The numbers in parentheses are obtained using the results on the fluoride complex only.

While the hydrogen-bond energies calculated at the MP2 level were quite close to those at the CCSD(T) level, the hydrogen-bond energies estimated using the DFT methods showed larger variations depending on the functionals employed, especially for the fluoride complex. *Table* 4 presents statistical deviations calculated on the hydrogen-

***Table* 5.** Harmonic and scaled frequencies in $cm^{-1}$ of HCCH

| Method | Scale factor | $\omega_1$ ($\sigma_g$) | $\omega_2$ ($\sigma_g$) | $\omega_3$ ($\sigma_u$) | $\omega_4$ ($\pi_g$) | $\omega_5$ ($\pi_u$) | RMSD |
|---|---|---|---|---|---|---|---|
| CCSD(T) | | 3503 | 1995 | 3395 | 593 | 749 | 65.1 |
| | 0.9710 | 3401 | 1937 | 3296 | 576 | 727 | 26.0 |
| MP2 | | 3534 | 1968 | 3432 | 601 | 754 | 82.1 |
| | 0.9645 | 3408 | 1898 | 3310 | 580 | 727 | 36.7 |
| B97-D | | 3459 | 2009 | 3357 | 609 | 747 | 44.1 |
| | 0.9790 | 3386 | 1966 | 3286 | 596 | 732 | 9.9 |
| B3LYP | | 3517 | 2068 | 3412 | 666 | 769 | 87.3 |
| | 0.9588 | 3372 | 1983 | 3272 | 639 | 738 | 16.6 |
| B3LYP-D3 | | 3514 | 2066 | 3409 | 667 | 770 | 85.9 |
| | 0.9596 | 3372 | 1983 | 3271 | 640 | 739 | 17.5 |
| PBE1PBE | | 3529 | 2080 | 3421 | 675 | 776 | 96.3 |
| | 0.9550 | 3370 | 1987 | 3267 | 645 | 741 | 20.7 |
| M06-2X | | 3535 | 2103 | 3421 | 707 | 790 | 110.4 |
| | 0.9507 | 3360 | 1999 | 3253 | 672 | 751 | 38.4 |
| CAM-B3LYP | | 3529 | 2103 | 3420 | 710 | 781 | 108.5 |
| | 0.9518 | 3359 | 2001 | 3255 | 676 | 744 | 39.1 |
| LC-ωHPBE | | 3536 | 2122 | 3422 | 746 | 794 | 125.6 |
| | 0.9470 | 3349 | 2010 | 3241 | 707 | 752 | 57.5 |
| LC-BLYP | | 3545 | 2152 | 3427 | 775 | 800 | 143.1 |
| | 0.9418 | 3339 | 2027 | 3228 | 730 | 754 | 72.6 |
| ωB97X-D | | 3529 | 2090 | 3420 | 694 | 780 | 102.3 |
| | 0.9534 | 3365 | 1992 | 3261 | 661 | 744 | 30.4 |
| Expt[a] | | 3374 | 1974 | 3289 | 612 | 730 | |

[a]Ref. 39.

bond energies using the CCSD(T) energies as reference. As in the analysis on geometrical parameters, separate deviations were also calculated with the results on the fluoride complex. Examining the results on all three anion complexes, the LC-ωHPBE functional was the best performer for the hydrogen-bond energies. The CAM-B3LYP and B97-D functionals showed relatively good performance although the results on the fluoride complex were not quite satisfactory. On the other hand, the PBE1PBE and M06-2X functionals gave rather poor performance, whose performance has been noted previously in the systems with non-bonded and hydrogen-bonding interactions.[35,36] We also note that the B3LYP functional yielded very close values to the CCSD(T) energies. This is a little surprising since the B3LYP functional is known to give unsatisfactory results for hydrogen-bond energies.[37,38]

***Table* 6.** Scaled harmonic frequencies in $cm^{-1}$ of the $X^-$–HCCH complexes (X = F, Cl, and Br)

| Method | $\omega_1$ ($\sigma_g$) | $\omega_2$ ($\sigma_g$) | $\omega_3$ ($\sigma_g$) | $\omega_4$ ($\sigma_g$) | $\omega_5$ ($\pi$) | $\omega_6$ ($\pi$) | $\omega_7$ ($\pi$) |
|---|---|---|---|---|---|---|---|
| | | | $F^-$–HCCH | | | | |
| CCSD(T) | 3296 | 1878 | 1497 | 295 | 1201 | 543 | 156 |
| MP2 | 3318 | 1864 | 800 | 292 | 1236 | 556 | 160 |
| B97-D | 3288 | 1949 | 503 | 444 | 1210 | 555 | 153 |
| B3LYP | 3302 | 2051 | 994 | 308 | 1188 | 588 | 177 |
| B3LYP-D3 | 3303 | 2058 | 1053 | 318 | 1185 | 590 | 178 |
| PBE1PBE | 3282 | 1954 | 935 | 365 | 1210 | 584 | 161 |
| M06-2X | 3269 | 1948 | 1703 | 345 | 1152 | 607 | 155 |
| CAM-B3LYP | 3295 | 2071 | 975 | 309 | 1197 | 613 | 187 |
| LC-ωHPBE | 3281 | 2065 | 847 | 322 | 1212 | 638 | 190 |
| LC-BLYP | 3282 | 2125 | 1166 | 317 | 1195 | 655 | 196 |
| ωB97X-D | 3282 | 1974 | 631 | 295 | 1221 | 594 | 169 |
| | | | $Cl^-$–HCCH | | | | |
| CCSD(T) | 3353 | 2963 | 1880 | 153 | 912 | 577 | 148 |
| MP2 | 3365 | 2946 | 1839 | 153 | 912 | 581 | 146 |
| B97-D | 3337 | 2877 | 1889 | 130 | 892 | 588 | 135 |
| B3LYP | 3330 | 2909 | 1917 | 138 | 904 | 621 | 140 |
| B3LYP-D3 | 3330 | 2912 | 1916 | 140 | 902 | 622 | 138 |
| PBE1PBE | 3326 | 2851 | 1909 | 149 | 919 | 627 | 144 |
| M06-2X | 3319 | 2925 | 1937 | 145 | 914 | 656 | 141 |
| CAM-B3LYP | 3318 | 2918 | 1939 | 141 | 915 | 650 | 144 |
| LC-ωHPBE | 3306 | 2911 | 1948 | 137 | 926 | 676 | 147 |
| LC-BLYP | 3300 | 2915 | 1968 | 146 | 934 | 691 | 147 |
| ωB97X-D | 3322 | 2913 | 1928 | 140 | 907 | 640 | 142 |
| Expt[a] | | 2938 | | | | | |
| | | | $Br^-$–HCCH | | | | |
| CCSD(T) | 3357 | 3023 | 1891 | 126 | 904 | 579 | 144 |
| MP2 | 3368 | 3009 | 1849 | 127 | 904 | 583 | 142 |
| B97-D | 3343 | 2991 | 1911 | 92 | 853 | 592 | 122 |
| B3LYP | 3333 | 2996 | 1932 | 103 | 870 | 626 | 129 |
| B3LYP-D3 | 3333 | 3000 | 1932 | 104 | 867 | 627 | 126 |
| PBE1PBE | 3329 | 2950 | 1928 | 111 | 883 | 631 | 132 |
| M06-2X | 3322 | 3012 | 1952 | 110 | 880 | 659 | 128 |
| CAM-B3LYP | 3322 | 3002 | 1954 | 105 | 882 | 655 | 132 |
| LC-ωHPBE | 3310 | 2996 | 1964 | 103 | 893 | 681 | 135 |
| LC-BLYP | 3303 | 2991 | 1982 | 109 | 902 | 696 | 135 |
| ωB97X-D | 3326 | 3001 | 1944 | 105 | 873 | 645 | 130 |
| Expt[b] | 3340 | 2981.28 | | | | | |

[a]Ref. 14a
[b]Ref. 15a.

Before determining vibrational frequencies of the halide-acetylene complexes, frequencies of the free acetylene molecule were calculated to determine the proper scale factor for each method. As shown in *Table* 5, the calculated harmonic frequencies of acetylene exhibited considerable deviations from the experimental frequencies,[39] and the root-mean-square deviations (RMSD) were quite large. Since the accurate experimental frequencies are available for acetylene,[39] the scale factors were determined for each method by minimizing the deviation of calculated harmonic frequencies from experiment in linear least-squares manner, and the resulting scale factors are presented in *Table* 5. After applying the scales factor, the deviation from the experimental values, and accordingly the RMSD value decreased considerably. The B97-D and B3LYP functionals, in particular, yielded very excellent results after scaling, leading to a better agreement than the *ab initio* CCSD(T) and MP2 methods.

*Table* 6 shows the scaled harmonic frequencies of the halide-acetylene complexes calculated at various levels along with the experimental frequencies available. Upon complexation of the acetylene molecule with halide ion, the symmetric and antisymmetric C–H stretch modes of acetylene transform into local modes, $\omega_1$ and $\omega_2$, that correspond to motion of the free and bound protons, respectively. For the fluoride complex, the frequency of the $\omega_3$ mode, which corresponds to H-F stretching motion in the complex, showed quite a large variation depending on the level of theory. This result, along with the result on the optimized geometry of the fluoride complex, suggests that the accurate description of the fluoride-acetylene complex is quite difficult and more careful study is needed. For the chloride and bromide complexes, the scaled frequencies obtained at various levels showed much smaller variations. For these anion complexes, a few experimental frequencies are available for the $\omega_1$ and $\omega_2$ modes from vibrational predissociation spectroscopy.[14,15] As shown in *Table* 6, the scaled frequencies are in reasonably good agreement with the experimental values.

*Table* 7 shows the statistical deviations calculated on the scaled harmonic frequencies of the halide-acetylene complexes. While the scaled MP2 frequencies were the closest to those of CCSD(T), density functionals examined here gave rather similar performance with slightly larger deviations compared to the MP2 method. The PBE1PBE, M06-2X, and B3LYP functionals yielded relatively small deviations compared to other functionals. However, the B3LYP functional has often shown better performance over the CCSD(T) method in estimating vibrational frequencies and related properties.[40,41] Therefore, statistical deviations calculated using CCSD(T) frequencies as reference in *Table* 7 may be misleading, and B3LYP frequencies may serve better as reference. When the statistical deviations were calculated relative to B3LYP frequencies as reference, the MAPD values were found to be small in the order of CAM-B3LYP (2.2%), ωB97X-D (2.9%), LC-ωHPBE (4.2%), and, PBE1PBE (4.3%) functionals.

***Table* 7.** Statistical analysis of the vibrational frequencies of $X^-$–HCCH relative to the CCSD(T) values

| Method | MAD ($cm^{-1}$) | MSD ($cm^{-1}$) | MAPD (%) |
|---|---|---|---|
| MP2 | 33.4 | –22.2 | 2.7 (6.5)[a] |
| B97-D | 58.9 | –36.1 | 8.4 (13.1) |
| B3LYP | 46.9 | –7.9 | 6.7 (9.3) |
| B3LYP-D3 | 46.4 | –5.6 | 7.0 (9.5) |
| PBE1PBE | 48.3 | –12.2 | 5.9 (8.8) |
| M06-2X | 41.8 | 17.9 | 6.3 (6.8) |
| CAM-B3LYP | 53.8 | 2.0 | 7.7 (11.6) |
| LC-ωHPBE | 66.2 | 4.9 | 9.2 (14.3) |
| LC-BLYP | 61.7 | 22.3 | 9.0 (13.7) |
| ωB97X-D | 59.5 | –17.8 | 7.2 (10.2) |

[a]The numbers in parentheses are obtained using the results on the fluoride complex only.

## CONCLUSION

In the present study, the halide-acetylene anion complexes have been investigated by using several different *ab initio* and DFT methods to characterize ionic hydrogen-bonded complexes and to assess the performance of various density functionals. The halide-acetylene complexes all have linear equilibrium structures. However, it was found that the fluoride complex behaves differently with the character of $[F\text{-}H\cdots CCH]^-$, while the chloride and bromide ions form hydrogen-bonded complexes with the acetylene molecule. The hydrogen-bond energies of the halide-acetylene anions were estimated with zero-point energy and BSSE corrections. Although for the fluoride complex, some variations in hydrogen-bond energies were observed depending on density functionals employed, the variations were much smaller for the chloride and bromide complexes. The vibrational frequencies of the anion complexes were estimated using scale factors determined based on the experimental frequencies for the free acetylene molecule. Although only a few experimental frequencies had been reported, the scaled harmonic frequencies for the complexes agreed quite well with the experimental frequencies available.

The performance of various density functionals employed in the present study was assessed by examining statistical deviations with respect to the *ab initio* CCSD(T) results. The density functionals employed in the present work showed quite different performances depending on the properties of interest. For the geometrical parameters related with hydrogen bonding, M06-2X produced the closest results to those predicted by the CCSD(T) method and to a lesser extent, PBE1PBE and ωB97X-D yielded closer results to CCSD(T). On the other hand, the LC-ωHPBE, CAM-B3LYP, and B97-D functionals were among the best performers for hydrogen-bond energies, but PBE1PBE and M06-2X yielded rather poor results. Density functionals examined in the present study gave rather similar performance for the vibrational frequencies, although the PBE1PBE, M06-2X, and B3LYP functionals yielded relatively smaller deviations from the CCSD(T) frequencies. The present study suggests that molecular structures and properties cannot be treated equally with a single density functional, but careful consideration is needed in choosing density functionals appropriate for the molecular property of interest.

**Acknowledgments.** This work was supported by Research Grant of Incheon National University in 2021 to B.-S. Cheong.

## REFERENCES

1. (a) Jeffrey, G. A. *An Introduction to Hydrogen Bonding*; Oxford University Press: Oxford, U. K., 1997; (b) Jeffrey, G. A.; Saenger, W. *Hydrogen Bonding in Biological Structures*; Springer, Berlin, Germany, 1991.
2. Desiraju, G. R.; Steiner, T. *The Weak Hydrogen Bond in Structural Chemistry and Biology*; Oxford University Press: Oxford, U. K., 1999.
3. (a) Meot-Ner, M. *Chem. Rev.* **2005**, *105*, 213. (b) Meot-Ner, M. *Chem. Rev.* **2012**, *112*, PR22.
4. Scheiner, S. *Hydrogen Bonding. A Theoretical Perspective*; Oxford University Press: Oxford, U. K., 1997.
5. Hadzi, D. Ed. Theoretical Treatments of Hydrogen Bonding; Wiley, Chichester, U. K., 1997.
6. Mardirossian, N.; Head-Gordon, M. *Mol. Phys.* **2017**, *115*, 2315.
7. DiLabio, G. A.; Otero-de-la-Roza, A. In *Reviews in Computational Chemistry*; Parrill, A. L.; Lipkowitz, K. B., Eds.; Wiley-Intersceince, **2016**, *29*, 1.
8. (a) Boese, A. D. *Chem. Phys. Chem.* **2015**, *16*, 978. (b) DiLabio, G. A.; Johnson, E. R.; Otero-de-la-Roza, A. *Phys. Chem. Chem. Phys.* **2013**, *15*, 12821. (c) Burns, L. A.; Vazquez-Mayagoitia, A.; Sumpter, B. G.; Sherrill, C. D. *J. Chem. Phys.* **2011**, *134*, 084107.
9. (a) Robertson, W. H.; Johnson, M. A. *Annu. Rev. Phys. Chem.* **2003**, *54*, 173. (b) Roscioli, J. R.; Diken, E. G.; Johnson, M. A.; Horvath, S.; McCoy, A. B. *J. Phys. Chem. A* **2006**, *110*, 4943. (c) Weis, P.; Kemper, P. R.; Bowers, M. T. *J. Am. Chem. Soc.* **1999**, *121*, 3531. (d) Hiraoka, K.; Mizuse, S.; Yamabe, S. *J. Phys. Chem.* **1988**, *92*, 3943.
10. (a) Choi, J. H.; Kuwata, K. T.; Cao, Y. B.; Okumura, M. *J. Phys. Chem. A*, **1998**, *102*, 503. (b) Ayotte, P.; Weddle, G. H.; Kim, J.; Johnson, M. A. *J. Am. Chem. Soc.* **1998**, *120*, 12361.
11. (a) Ayotte, P.; Bailey, C. G.; Weddle, G. H.; Johnson, M. A. *J. Phys. Chem.* **1998**, *102*, 3067. (b) Chaban, G. M.; Xantheas, S. S.; Gerber, R. G. *J. Phys. Chem. A* **2003**, *107*, 4952.
12. (a) Masamura, M. *J. Phys. Chem. A* **2002**, *106*, 8925. (b) Masamura, M. *J. Chem. Phys.* **2003**, *118*, 6336. (c) Xantheas, S. S.; Dang, L. X. *J. Phys. Chem.* **1996**, *100*, 3989. (d) Xantheas, S. S. *J. Phys. Chem.* **1996**, *100*, 9703.
13. Cheong, B. S. submitted for publication.
14. (a) Weiser, P. S.; Wild, D. A.; Bieske, E. J. *J. Chem. Phys.* **1999**, *110*, 9443; (b) Wild, D. A.; Loh, Z. M.; Wilson, R. L.; Bieske, E. J. *Chem. Phys. Lett.* **2003**, *369*, 684.
15. (a) Wild, D. A.; Milley, P. J.; Loh, Z. M.; Wolynec, P. P.; Weiser, P. S.; Bieske, E. J. *J. Chem. Phys.* **2000**, *113*, 1075; (b) Wild, D. A.; Milley, P. J.; Loh, Z. M.; Weiser, P. S.; Bieske, E. J. *Chem. Phys. Lett.* **2000**, *323*, 49.
16. Weiser, P. S.; Wild, D. A.; Bieske, E. J. *Chem. Phys. Lett.* **1999**, *299*, 303.
17. Beckham, D. A. R.; Conran, S.; Lapere, K. M.; Kettner, M.; McKinley, A. J.; Wild, D. A. *Chem. Phys. Lett.* **2015**, *619*, 241.
18. (a) Botschwina, P.; Dutoi, T.; Mladenovic, M.; Oswald, R.; Schmatz, S.; Stoll, H. *Faraday Discuss.* **2001**, *118*, 433; (b) Botschwina, P.; Oswald, R. *J. Chem. Phys.* **2002**, *117*, 4800.
19. Botschwina, P.; Stoll, H. *Phys. Chem. Chem. Phys.* **2001**, *3*, 1965.
20. Denis, P. A.; Gancheff, J. S. *Struct. Chem.* **2014**, *25*, 903.
21. Becke, A. D. *J. Chem. Phys.* **1997**, *107*, 8554.
22. Stephens, P. J.; Devlin, F. J.; Chabalowski, C. F.; Frisch, M. J. *J. Phys. Chem.* **1994**, *98*, 11623, and references therein.
23. Adamo, C.; Barone, V. *J. Chem. Phys.* **1999**, *110*, 6158.
24. Zhao, Y.; Truhlar, D. G. *Theor. Chem. Acc.* **2008**, *120*, 215.
25. Yanai, T.; Tew, D.; Handy, N. *Chem. Phys. Lett.* **2004**, *393*, 51.
26. (a) Henderson, T. M.; Izmaylov, A. F.; Scalmani, G.; Scuseria, G. E. *J. Chem. Phys.* **2009**, *131*, 044108. (b) Vydrov, O. A.; Heyd, J.; Krukau, A.; Scuseria, G. E. *J. Chem. Phys.* **2006**, *125*, 074106. (c) Vydrov, O. A.; Scuseria, G. E. *J. Chem. Phys.* **2006**, *125*, 234109.
27. (a) Chai, J.-D.; Head-Gordon, M. *J. Chem. Phys.* **2008**, *128*, 084106. (b) Chai, J.-D.; Head-Gordon, M. *Phys. Chem. Chem. Phys.* **2008**, *10*, 6615.
28. Iikura, H.; Tsuneda, T.; Yanai, T.; Hirao, K. *J. Chem. Phys.* **2001**, *115*, 3540.
29. (a) Grimme, S. *J. Comp. Chem.* **2006**, *27*, 1787. (b) Grimme, S.; Antony, J.; Ehrlich, S.; Krieg, H. *J. Chem. Phys*. **2010**,

*132*, 154104.
30. Boys, S. F.; Bernardi, F. *Mol. Phys.* **1970**, *19*, 553.
31. Pudzianowski, A. T. *J. Chem. Phys.* **1995**, *102*, 8029.
32. (a) Martin, J. M. L.; Oliveira, G. de *J. Chem. Phys.* **1999**, *111*, 1843. (b) Barnes, E. C.; Petersson, G. A.; Montgomery, J. A.; Frisch, M. J.; Martin, J. M. L. *J. Chem. Theory Comput.* **2009**, *5*, 2687.
33. Curtiss, L. A.; Redfern, P. C.; Raghavachari, K. *J. Chem. Phys.* **2007**, *126*, 084108.
34. Frisch, M. J.; Trucks, G. W.; Schlegel, H. B.; Scuseria, G. E.; Robb, M. A.; Cheeseman, J. R.; Scalmani, G.; Barone, V.; Petersson, G. A.; Nakatsuji, H.; Li, X.; Caricato, M.; Marenich, A. V.; Bloino, J.; Janesko, B. G.; Gomperts, R.; Mennucci, B.; Hratchian, H. P.; Ortiz, J. V.; Izmaylov, A. F.; Sonnenberg, J. L.; Williams-Young, D.; Ding, F.; Lipparini, F.; Egidi, F.; Goings, J.; Peng, B.; Petrone, A.; Henderson, T.; Ranasinghe, D.; Zakrzewski, V. G.; Gao, J.; Rega, N.; Zheng, G.; Liang, W.; Hada, M.; Ehara, M.; Toyota, K.; Fukuda, R.; Hasegawa, J.; Ishida, M.; Nakajima, T.; Honda, Y.; Kitao, O.; Nakai, H.; Vreven, T.; Throssell, K.; Montgomery, Jr., J. A.; Peralta, J. E.; Ogliaro, F.; Bearpark, M. J.; Heyd, J. J.; Brothers, E. N.; Kudin, K. N.; Staroverov, V. N.; Keith, T. A.; Kobayashi, R.; Normand, J.; Raghavachari, K.; Rendell, A. P.; Burant, J. C.; Iyengar, S. S.; Tomasi, J.; Cossi, M.; Millam, J. M.; Klene, M.; Adamo, C.; Cammi, R.; Ochterski, J. W.; Martin, R. L.; Morokuma, K.; Farkas, O.; Foresman, J. B.; Fox, D. J. *Gaussian 16*, *Revision C.01*, Gaussian, Inc.: Wallingford, CT, **2019**.
35. Zhao, Y.; Truhlar, D. G. *J. Chem. Theory Comput*. **2005**, *1*, 415.
36. Walker, M.; Harvey, A. J. A.; Sen, A.; Dessent, C. E. H. *J. Phys. Chem. A* **2013**, *117*, 12590.
37. Rao, L.; Ke, H.; Fu, G.; Xu, X.; Yan, Y. *J. Chem. Theory Comput.* **2009**, *5*, 86.
38. Tuma, C.; Boese, A. D.; Handy, N. C. *Phys. Chem. Chem. Phys.* **1999**, *1*, 3939.
39. Shimanouchi, T. *Tables of Molecular Vibrational Frequencies Consolidated Volume I*, National Bureau of Standards, 1972.
40. (a) Barone, V. *J. Phys. Chem A* **2004**, *108*, 4146. (b) Barone, V. *Chem. Phys. Lett.* **2004**, *383*, 58.
41. Puzzarini, C.; Biczysko, M.; Barone, V. *J. Chem. Theory Comput.* **2010**, *6*, 828.